Waves and turbulence in magnetohydrodynamic direct numerical simulations

Pablo Dmitruk[1] and W. H. Matthaeus[2]
[1]*Departamento de Física, Facultad de Ciencias Exactas y Naturales, Universidad de Buenos Aires, Ciudad Universitaria, 1428 Buenos Aires, Argentina*
[2]*Department of Physics and Astronomy and Bartol Research Institute, University of Delaware, Newark, Delaware 19716, USA*

(Received 25 March 2009; accepted 8 May 2009; published online 3 June 2009)

Direct numerical simulations of the incompressible MHD equations with a uniform background magnetic field in a turbulent regime are performed to assess the relative importance of broadband turbulent fluctuations and wavelike fluctuations that are associated with an Alfvén wave dispersion relation. The focus is on properties of the fluctuations in the frequency domain. Eulerian frequency spectra and individual wave number mode frequency spectra show the presence of peaks at the corresponding Alfvén wave frequencies for full nonlinear simulations in a turbulent regime. The peaks are however broad and their power content is compared to the power in the full spectrum as well as a signal to noise ratio is defined and quantified for different values of the background magnetic field. The ratio of power in Alfvén waves to the power in the rest of the spectrum is also quantified and is found to be small for different values of the mean magnetic field. Individual modes in time show a much more complex behavior than that could be expected for linear solutions. Also, nonlinear transfer of energy is evidenced by the existence of peaks at wave numbers perpendicular to the mean magnetic field. Implications are discussed for theories of strong turbulence as well as perturbation theories that assume the leading order behavior is that of propagating Alfvén waves.
 [DOI: 10.1063/1.3148335]

I. INTRODUCTION

It is well known that magnetohydrodynamics (MHD), in the linear approximation, supports the existence of a number of waves, each of which is associated with a dispersion relation that relates frequency to wave number. The simplest case corresponds to incompressible MHD with a uniform background magnetic field $\mathbf{B_0}$, for which the linear dispersion relation (in the ideal nondissipative case) describes Alfvén waves, with frequency $w=\mathbf{k}\cdot\mathbf{v_A}$, for wave vector $\mathbf{k}$, Alfvén velocity $\mathbf{v_A}=\mathbf{B_0}/\sqrt{4\pi\rho}$, and density ρ. The complex Fourier components of velocity $\mathbf{v_k}$ and magnetic field fluctuation $\mathbf{b_k}$ are transverse to the wave vector, $\mathbf{v_k}\cdot\mathbf{k}=\mathbf{b_k}\cdot\mathbf{k}=0$.[1]

On the other hand, when nonlinear terms are taken into account, the MHD equations develop a turbulent regime, characterized by a broad range of length scales and correspondingly time scales. In the turbulent regime however one does not expect a direct or explicit relation between frequency and wave number, such as the dispersion relation for waves. Commonly, for instance in observational studies of MHD plasmas such as the solar wind,[2] the observed frequency spectra is assumed to be related to wave number spectra through a frozen-in flow hypothesis (the solar wind flow velocity acting as the proportionality constant). The Eulerian frequency spectrum, transform of the single-point, multiple time correlation function[3] is not directly measured. Nevertheless there is no evidence in the form of the observed interplanetary spectra that suggests a role of a dispersion relation.

The observation of Alfvénic correlations in the solar wind[4–6] is reminiscent of a particular special case, in which waves can be an exact solution of the full, large amplitude, nonlinear MHD equations. These correspond to situations in which the MHD velocity fluctuations are exactly parallel to (or antiparallel to) and in energy equipartition with the magnetic field fluctuations. When the magnetic field is in familiar Alfvén speed units, this condition is simply $\mathbf{v}=\pm\mathbf{b}$. The solution is then a large amplitude Alfvén wave packet. This type of wave packet will propagate unidirectionally along (or antiparallel to) a uniform mean field, if one is present; however, this "Alfvénic" solution is obtained equally well with no mean field.[7] It is important to recognize that this large amplitude wave solution does not satisfy a general superposition principle, wave packets with opposite senses of $\mathbf{v}-\mathbf{b}$ correlation,[8] when overlapping in space, no longer propagate without distortion.[9] Instead, turbulence develops and one can ask to what extent the wave description is still useful in that regime. In other words, it is still possible to talk about waves in a turbulent regime? Or, a related question, can we still distinguish some wave activity in a turbulent regime? It is these issues that we address here.

There is no analog to these questions in standard homogeneous incompressible hydrodynamic turbulence, because wave modes are lacking. However in studies of MHD, the possibility of a leading order wave description arises, and indeed this is assumed in a variety of theories that are generically known as "weak turbulence."[10,11] In fact, the interplay of waves and turbulent fluctuations (nonlinear activity) is actually a complex topic in MHD (Ref. 12) where it was pioneered by the works by Kraichnan,[9] as well as in the

general context of plasma physics.[13] Indeed, much of the subject of MHD turbulence is permeated by discussion of the balance of wavelike and nonlinear activity.

To study these issues, we will consider here a simple model, for which answers to the key questions regarding the role of waves can be obtained quantitatively: incompressible MHD with a uniform background magnetic field, and periodic boundary conditions in a rectangular box. Direct numerical solutions of the nonlinear MHD equations will be obtained for different cases, with the purpose of comparing mainly the results in the frequency domain and to see to what extent waves can still be distinguished once a turbulent regime is developed. Unlike the usual study of wave number spectrum in MHD, we will look at frequency spectra obtained from time series of the magnetic field fluctuations at distributed probes in the simulation, and also frequency spectra for time series of individual wave number modes. The influence of the value of the background magnetic field on the results will be analyzed through a series of simulations in which this parameter is varied. In particular, for a specific set of numerical experiments, we will examine quantitatively the familiar heuristic notion that when "$\delta B/B$," the ratio of fluctuating magnetic field to mean magnetic field, goes to zero, the MHD behavior becomes ever more wavelike.

II. EQUATIONS, NUMERICAL SIMULATIONS, AND DIAGNOSTICS

The incompressible MHD equations (momentum and induction equations) in dimensionless units are

$$\frac{\partial \mathbf{v}}{\partial t} + \mathbf{v}\cdot\nabla\mathbf{v} = -\frac{1}{\rho}\nabla p + \mathbf{j}\times\mathbf{B} + \frac{1}{R}\nabla^2\mathbf{v}, \tag{1}$$

$$\frac{\partial \mathbf{b}}{\partial t} = \nabla\times(\mathbf{v}\times\mathbf{B}) + \frac{1}{R_m}\nabla^2\mathbf{b}, \tag{2}$$

where $\mathbf{v}$ is the plasma velocity, $\mathbf{B}=\mathbf{b}+\mathbf{B_0}$ is the magnetic field, with a fluctuating part $\mathbf{b}$ and a mean field (dc field) $\mathbf{B_0}$, $\mathbf{j}=\nabla\times\mathbf{b}$ is the current density, p is the pressure, and ρ is the plasma density. The units are based on a characteristic speed v_0, which for MHD is chosen to be the typical Alfvén speed of the magnetic field fluctuations, $v_0=v_a=\langle b^2\rangle^{1/2}/\sqrt{4\pi\rho}$. The characteristic length scale is L where the simulation box side length is defined as $2\pi L$. The unit time is $t_0=L/v_0$, which for MHD becomes the Alfvén crossing time. The dimensionless parameters appearing in the equations are the kinetic and magnetic Reynolds numbers $R=v_0L/\nu$, $R_m=v_0L/\mu$ (with ν the kinematic viscosity and μ the magnetic diffusivity).

Equations (1) and (2) are solved with a triply periodic Fourier pseudospectral code. Results are reported here from runs with resolution of 128^3 grid points that allow very long time integrations to obtain well resolved frequency power spectra. The large scale Reynolds numbers are $R=R_m=400$. The scheme ensures exact energy conservation for the continuous time, spatially discrete equations. The discrete time integration is done with a second-order Runge–Kutta method. The method ensures stabilized aliasing errors.

The initial state consists of nonzero fluctuation amplitudes for the velocity and magnetic field (in equipartition and with total mean squares normalized to 1) random phased in the k-space (wave vector) shell $1\le|\mathbf{k}|\le 4$ (with k in units of $1/L$). The initial cross helicity $H_c=\langle\mathbf{v}\cdot\mathbf{b}\rangle$ and magnetic helicity $H_m=\langle\mathbf{a}\cdot\mathbf{b}\rangle$ (with $\mathbf{a}$ as the potential vector for the fluctuating magnetic field) are small.

Driving terms are added to Eqs. (1) and (2) to achieve a statistically steady state. This requires that we integrate the equations for hundreds or thousands of characteristic nonlinear times. The driving consists of independent vector forcing terms $\mathbf{f}_v$, $\mathbf{f}_b$ for the velocity and magnetic field evolution equations. The forcing is k-dependent (only a range of modes are forced, with wave number between $k=1$ and $k=2$), with uncorrelated random intensities for each component at each time step and a memory function, which implies a controlled correlation time of the driving. The forcing correlation time is set up to be of the order of the unit time. The uncorrelated random intensities of the forcing components assure no systematic statistical injection of cross helicity or magnetic helicity. In general in these simulations the energy reaches a time-varying quasisteady level after tens of nonlinear times. The presence of low frequency fluctuations in some runs (see Ref. 14) imposes a requirement of very long run times, as we will discuss below.

Probes are put in the simulation box, meaning that we record at selected spatial positions the time series of the fluctuating magnetic field or velocity field. Specifically a plane is chosen in the middle of the simulation box and a set of 64 probes is placed in that plane in a regular array of 8×8 points. A similar procedure was employed in Ref. 15 to study the presence of discrete modes within a turbulent system. Long time series of the single point data are obtained (2000 unit times duration) to compute the Eulerian frequency power spectra at the position of each probe. All spectra are computed from one Cartesian component of the fluctuation time series. For cases with a mean magnetic field, this component is perpendicular to the mean field direction. Sampling rate of the time series (not to be confused with the much smaller time integration step in the simulation) is $\Delta t=0.04$ unit times, which is 25 samples per unit time. This corresponds to a Nyquist angular frequency of $\pi/\Delta t\approx=78$ in simulation units. The square absolute value of the complex fast Fourier transform of the time series is used to compute the power spectrum. An average spectrum is constructed using the spectra from all probes. This improves the statistics and reduces noise, especially at high frequencies.

III. EULERIAN FREQUENCY SPECTRA

We carried out driven, dissipative spectral method simulations of incompressible MHD with a uniform background magnetic field. The Eulerian frequency spectra were computed over very long times as described above.

Figure 1 shows the results for a case with a fixed uniform background magnetic field of $B_0=8$ and initial fluctuation amplitude of $\langle b^2\rangle^{1/2}=1$. This could be viewed as an example of moderately strong mean magnetic field, and therefore a good candidate for observing Alfvén wave behavior, and signatures of the associated wave dispersion relation. The full incompressible nonlinear MHD equations are

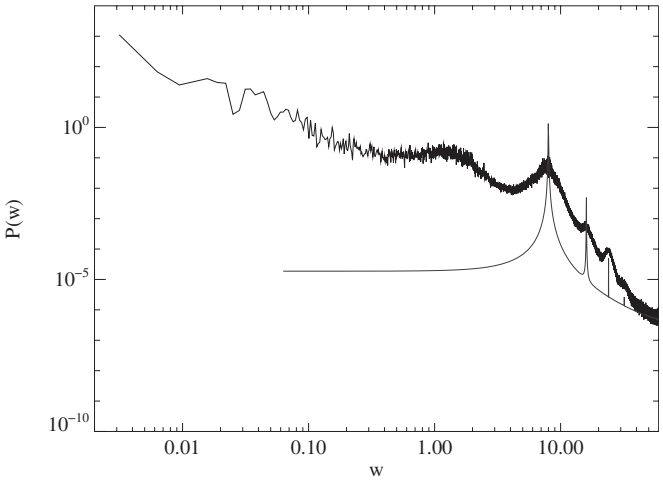

FIG. 1. Eulerian frequency spectra from MHD simulations. The frequency spectrum of magnetic field fluctuations δB (specifically b_x) from a full nonlinear solution of MHD with a background magnetic field $B_0=8\,\delta B$. In gray, the spectrum from a linear solution of the MHD equations, with no forcing or dissipation.

evolved for a long period of 2000 unit times. The driven system achieves an (statistically) stationary state after a few tens of unit times. The figure shows the Eulerian frequency spectrum for this case. A broadband frequency spectrum is obtained, with some (broad) peaks at particular frequencies. Also shown for reference is the spectra obtained if the MHD equations are solved using the same initial conditions, but with no forcing and dissipation, and putting the nonlinear terms to zero. The equations in this case are, of course, the linear system and the expected solutions are Alfvén waves of exact frequencies $w=\mathbf{k}\cdot\mathbf{v_A}=k_\parallel B_0$, which for $B_0=8$ correspond to peaks in the frequency spectrum at $w=8,16,24,\cdots$ (corresponding to $k_\parallel=1,2,3,\cdots$). The linearized case shows strong peaks at solutions to the dispersion relation, with these resonances broadened due to the finite integration time. In contrast, the full nonlinear solution shows a clearly broader frequency distribution. The peaks at the Alfvén waves can still be identified, although they are much broader and less dominant than in the linear case.

Other features of the observed broad band spectrum can also be understood. The spectrum of the driving is of the form $P(w)\sim 1/(w^2+w_c^2)$, with $w_c=1/\tau_c$, where τ_c is the (single) forcing correlation time. Here we set $t_c\sim 0.3$ so the spectrum of the driving is flat for frequencies $w<w_c\sim 3$ and is of the form $P(w)\sim w^{-2}$ for $w\gg w_c$. A spectral distribution near this form is visible at the intermediate and large frequencies in the spectrum of the nonlinear solution in Fig. 1 and may be due in part to forcing. It may also be in part associated with nonlinear couplings, which are expected to produce inertial range spectra in the range from $w^{-5/3}$ to w^{-2} at $w\gg 1$.[16,17] At the lower frequencies ($w\ll 1$) a power law spectrum is observed (rather than a flat spectrum associated with uncorrelated events). This power law behaves approximately as $P(w)\sim w^{-1}$. Such a feature is present sometimes in nonlinear solutions and is an instance of so-called "$1/f$ noise." Here, in MHD turbulence, this behavior becomes more evident for a large background magnetic field, as we discussed in more detail in a previous work.[14] A discussion of the influence of the mean magnetic field strength, along with a quantitative assessment of the importance of the wave power peaks, is given in Sec. IV.

IV. INFLUENCE OF THE MEAN MAGNETIC FIELD

We study the influence of the mean magnetic field by performing simulations with different values of $B_0=0,1,2,8,16$, while maintaining a fixed level of fluctuations $\delta B\sim 1$. All cases are driven to a statistically steady state using identical forcing algorithms. The results for the Eulerian frequency power spectrum are shown in Fig. 2. It can be seen that the Alfvén wave peaks become more distinct as the value of the mean magnetic field is increased. This might be expected, since the linearization to obtain the wave solution is typically connected to the limit $\delta B\ll B_0$. It is interesting that very little evidence of waves peaks can be seen for values of the mean field $B_0\leq 2$. Only a small peak corresponding to the lowest $k_\parallel=1$ mode ($w=B_0$) is observed for $B_0\leq 2$, while harmonic peaks at larger $k_\parallel$ modes can be seen only for the stronger mean field $B_0=8,16$ cases. Evidently the remainder of the frequency spectrum, the part that is not associated with the linearized solutions, is strong enough to obscure some of the periodic features expected from the dispersion relation in the low amplitude case. This broadband noise, a basic feature of turbulence, appears to dominate over much of the frequency range of the computed spectra.

It is of central relevance to develop a quantitative understanding of this mixture of turbulence and wave effects in the spectra. One such quantitative measure is a signal-to-noise-ratio (SNR) defined as[18]

$$\mathrm{SNR}=\log_{10}\left[\frac{P(w_0)}{P_0(w_0)}\right]. \tag{3}$$

Here w_0 is the frequency at the peak (center), corresponding to the Alfvén wave frequency, e.g., $w_0=B_0$ for $k_\parallel=1$, and $P_0(w_0)$ is a background value of the power spectrum, the value of the power spectrum $P(w)$ if the power law were continued through w_0, ignoring the peak at the wave frequency. The meaning of these parameters is illustrated in Fig. 3.

The SNR values for different values of B_0 are shown in Table I. This quantity is 0 for $B_0=0$ and increases monotonically to ~ 3 for the largest value considered $B_0=16$. The fact that the peaks are more noticeable for the large values of B_0 (see Fig. 2) is reflected then through this quantity. A conclusion could be drawn then that the waves dominate the picture as the value of B_0 is increased. This is certainly true for frequencies around the corresponding Alfvén wave frequencies. However, this quantity is local, in that it compares the spectral power in the waves only relative to the signal nearby in frequency.

The situation is different with regard to the total spectral power. The panels of Fig. 2 show that the spectral density is maximal at the lowest frequencies in all cases. Furthermore, this very low frequency power at $w<1$ represents an increasing fraction of the total spectral power for the larger values

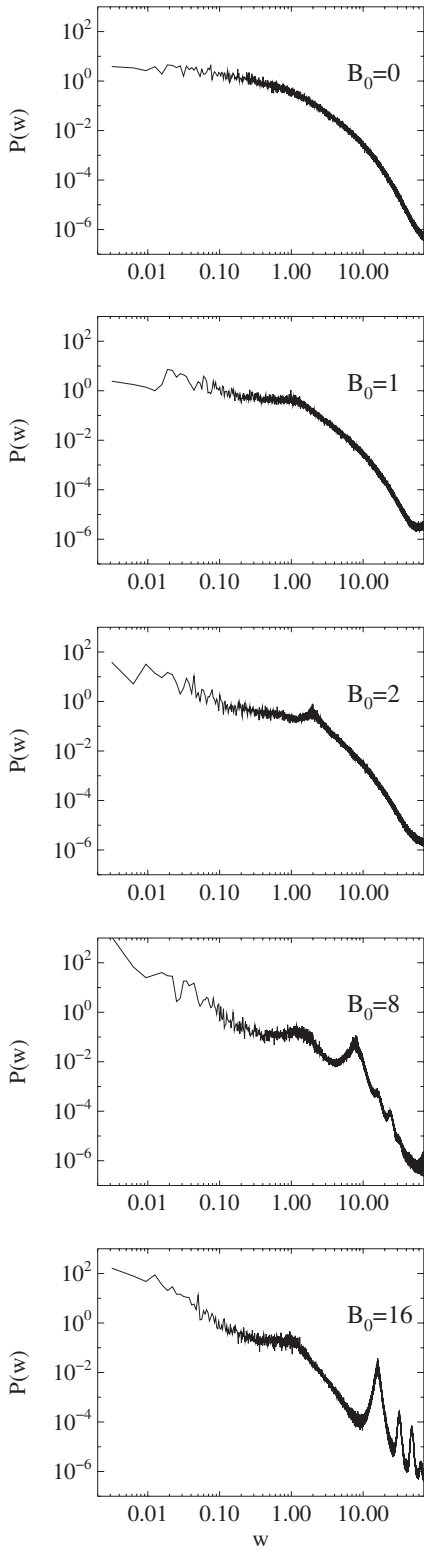

FIG. 2. Eulerian frequency spectra from full nonlinear solutions of the MHD equations for different values of the background magnetic field B_0.

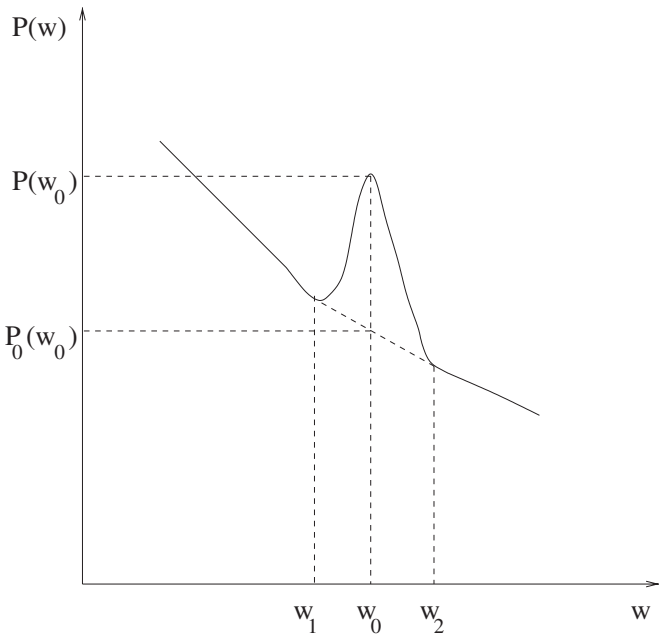

FIG. 3. Scheme for illustrating the different frequencies and power values around a peak of the power frequency spectrum.

$$\mathrm{WPR} = \frac{\int_{w_1}^{w_2}[P(w) - P_0(w)]dw}{\int_{w>0}P(w)dw}, \tag{4}$$

where w_1 and w_2 are values below and above the wave frequency peak w_0, as illustrated in Fig. 3. The values of the WPR for different values of B_0 are reported in Table I.

As can be seen in Table I, the fraction of power in the waves is as small as 2% for the largest value of B_0. It reaches its maximum (13%) for $B_0=2$. It is always a small fraction of the total power. Perhaps unanticipated from a wave perspective is that the wave power fraction again decreases at values of B_0 greater than $B_0=2$. This is due to an increase, as B_0 increases, in the importance of very low frequency power at frequencies much less than any of the discrete Alfvén wave frequencies. This can be seen in Fig. 2.

The origin of the power at low frequencies is not from any kind of wave but rather from fluctuations whose Fourier wave vectors **k** are mainly perpendicular to the mean magnetic field (i.e., small $k_\parallel$ or $k_\parallel=0$ fluctuations). This is a manifestation in the frequency domain of the well known spectra anisotropy of MHD under the influence of a strong uniform background magnetic field. Spectral anisotropy is familiar in MHD simulations,[19,20] is measured in laboratory experiments,[21] and has a number of manifestations in solar

of B_0. To demonstrate this quantitatively, another quantity can be defined, as a wave power ratio (WPR). This measure is the ratio of the power around the peak values (less the background spectrum if a power law would be continued) relative to the total power in all frequencies. This quantity is

TABLE I. SNR and WPR for different values of B_0.

B_0	SNR	WPR
0	0	0
1	0.3	0.1
2	0.6	0.13
8	1.5	0.03
16	3.1	0.02

wind fluctuations.[22] The common feature in all these cases is a suppression of excitation of high parallel wave vectors, due to an anisotropic cascade, so that much of the energy resides in very small parallel wave numbers, and $k_\perp \gg k_\parallel$ in the inertial cascade range. Such fluctuations, with wave vectors essentially perpendicular to the mean magnetic field, have near-zero frequency compared to the same wavelength mode with wave vector parallel to the mean field. (These fluctuations should not be called waves, in the sense that the term is applied to Alfvén waves with wave vectors parallel to the magnetic field.)

The frequency spectrum, as can be seen in Fig. 2, has a power law form at the lowest frequencies, especially for the large B_0 cases. This power law is of the form $P(w) \sim w^{-1}$, as we studied in more detail in a previous publication.[14] As reported there, the origin of the $1/w$ fluctuations is in nonlocal interactions of the lowest wave number modes $(k=1)$ with large k wave numbers. A recent study of nonlocal versus local interactions in decaying MHD with a strong magnetic field has been performed in Ref. 23. Evidently it is the enhancement of the low frequency $1/w$ power as B_0 becomes large that is responsible for the decrease in the fraction of power in identifiable wave modes in that same limit.

The evolution in time of a component of the magnetic field also shows some interesting features that are related to the above discussion. Figure 4 illustrates the full time evolution (2000 time units) of a component of the magnetic field (b_x), measured at a single fixed probe in the simulation. This is the counterpart, in the time domain, of the frequency plots in Fig. 2. A trend is clearly observed in the panels of Fig. 4 for different values of the mean magnetic field B_0. Together with the rapid fluctuations associated with Alfvén waves, conspicuous longer period fluctuations can be seen, and these become more conspicuous as the mean magnetic field is increased. A smaller time interval of 100 unit times is shown in Fig. 5 to appreciate in more detail this behavior. These long period fluctuations are the manifestation of the low-frequency activity visible in the power spectrum plots and specifically are associated with the $1/w$ power spectral feature as the mean magnetic field is increased. When sampled for an insufficiently long time period, the $1/w$ noise has the character of a time-varying mean magnetic field. Nevertheless it is truly low frequency turbulence, as it is generated entirely by nonlinear interactions.

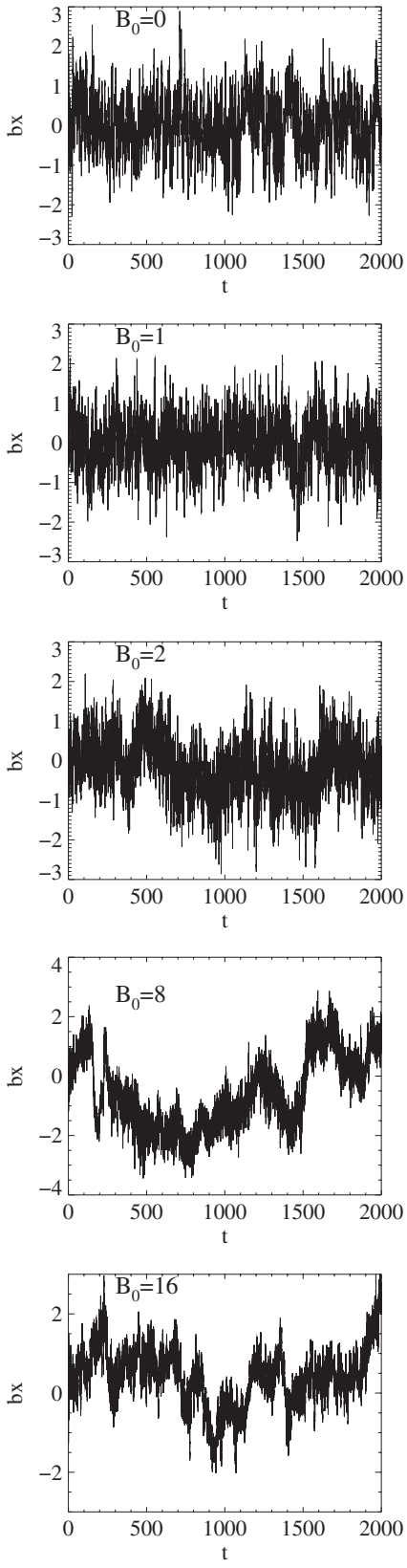

FIG. 4. Behavior in time for a component of the magnetic field at a single probe for different values of the background magnetic field.

V. FREQUENCY SPECTRA OF INDIVIDUAL MODES

A frequency power spectrum is computed for different single **k** modes. This is obtained from the complex time series of a mode $\mathbf{b}_\mathbf{k}(t)$, by computing the square absolute value of the fast Fourier transform of this time series. In this case, the time series is subdivided in periods and the frequency spectrum of each period is taken and then an average spectrum is constructed. This is done to improve the statistics and due to the fact that only one time series per wave number mode is obtained from a simulation. In contrast, for the case of the Eulerian spectrum in Sec. IV, many probes are used instead to improve the statistics.

Some sample results for individual mode frequency spectra are shown in Fig. 6. Panel (a) corresponds to the frequency spectra of several modes with $k_x=k_z=0$ and $k_y=1,2,4,8$. The mean magnetic field is in the y-direction,

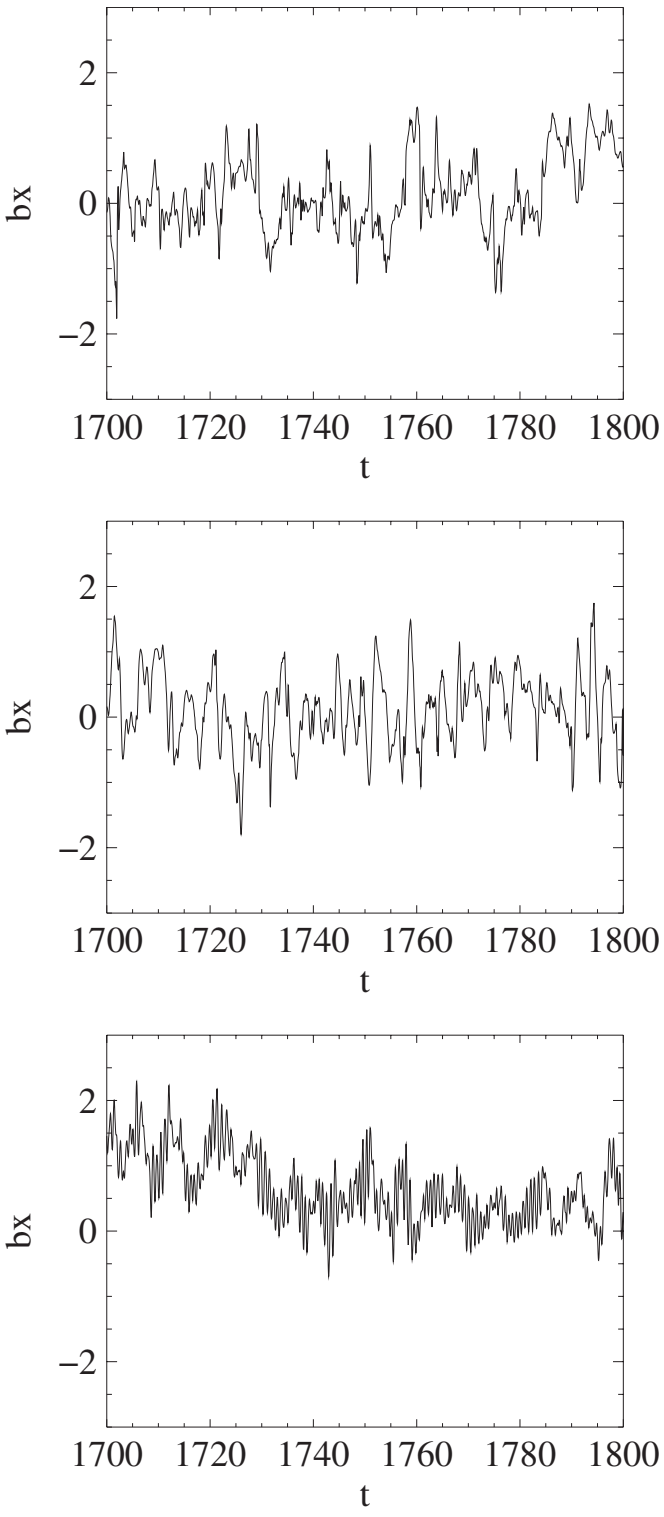

FIG. 5. Magnetic field component at a single probe, as in Fig. 4, but over a smaller time scale. A period of 100 unit times is shown for three different values of the background magnetic field to observe simultaneous existence of waves and longer time fluctuations.

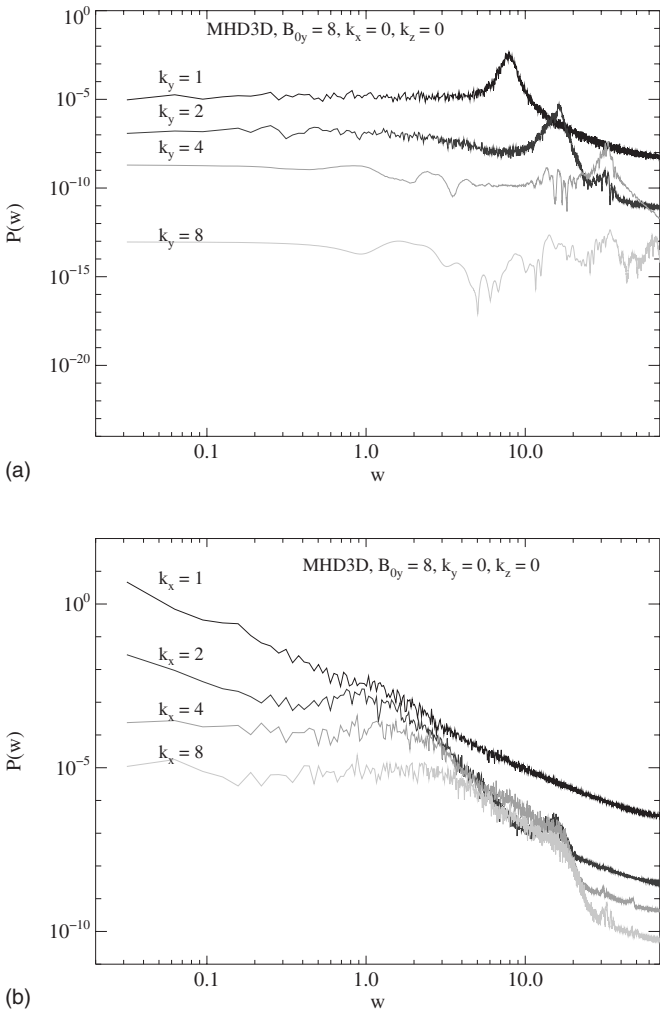

FIG. 6. Frequency spectra of individual wave number modes: (a) the spectra of modes with wave number parallel to the background magnetic field and (b) the spectra of modes with wave number perpendicular to the background magnetic field.

so these are purely "parallel" modes with $k=k_{\parallel}=k_y$. Such modes are intuitively "Alfvén waves," and in linear theory would have wave frequencies $w=8,16,32$, respectively, corresponding to the simulation value of the mean magnetic field, $B_0=8$. In fact, Fig. 6 demonstrates the presence of several peaks at the expected linear mode frequencies, indicating a degree of Alfvén wavelike features. We also see that the peaks that are present are broadened peaks in each wave number mode frequency spectrum. Note the similarity of the peak structure in Figs. 1 and 6 (the Eulerian spectrum), except that the individual mode spectra in panel (a) of Fig. 6, which are purely parallel ($k_{\perp}=0$), lack the low frequency power enhancement discussed in Sec. IV.

Even though point spectral features reminiscent of waves are present in the single mode frequency spectra, it is also clear that these modes do not behave as single waves but respond to the dynamics with a broad frequency spectrum. The $k_y=1$ mode corresponds to a directly driven mode and its overall intensity, as well as its wave intensity, is the highest of the spectra shown in panel (a) of Fig. 6. The other modes ($k_y=2,4,8$) arise in these runs only due to the nonlinear transfer of energy (cascade), but the presence of wave activity nonetheless can be seen in their spectra. The power at these larger k modes is smaller. Interestingly, the high wave number modes do not show a stronger wave spectral feature—a result that is counterintuitive but clearly associ-

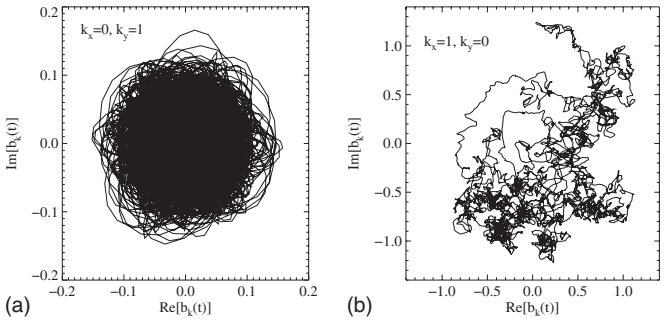

FIG. 7. Time behavior of individual wave number modes in the complex plane from the full nonlinear solution of the MHD equations: (a) the behavior of the $\mathbf{k}=(0,1,0)$ mode parallel to the background magnetic field and (b) the behavior of the $\mathbf{k}=(1,0,0)$ mode perpendicular to the background magnetic field.

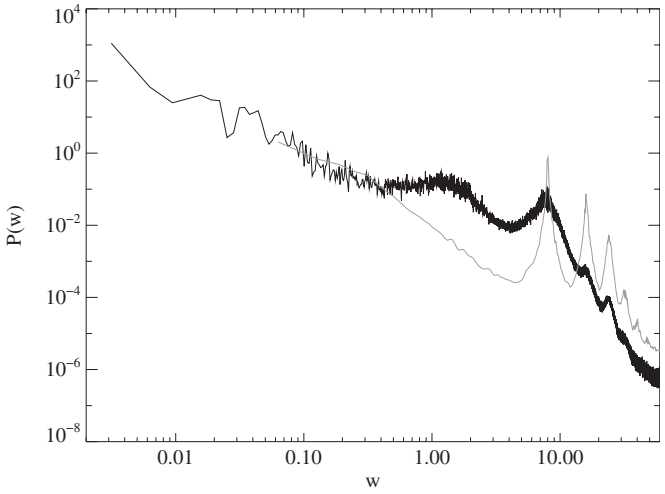

FIG. 8. Eulerian frequency spectrum for an undriven run (initial value problem) with $B_0=8$ and initial unit fluctuation energy. To render the time series stationary, the amplitude is scaled (normalized) by the square root of the energy at each time prior to computing the Fourier transform and the frequency spectrum. The resulting spectrum (thin line) is compared with the corresponding driven case (thick line) with $B_0=8$ discussed above (see Fig. 1).

ated with the strong nonlinear cascade effects experienced by these modes.

Panel (b) of Fig. 6 shows the frequency spectra of modes with $k_y=k_z=0$ and $k_x=1,2,4,8$. These are modes with wave vector purely perpendicular to the direction of the mean magnetic field, having $k_\parallel=0$. The Alfvén wave dispersion relation would indicate a frequency $w=0$ for these modes (since $k_\parallel=0$). Although their spectra are broadband, much of the power in the frequency spectrum of these modes is concentrated toward the lowest frequencies. An interesting feature is that there are some visible peaks at around $w=16$ for the three spectra with $k_x=2,4,8$. The origin of this peak can be readily understood through examination of the nonlinear couplings that occur involving triads of wave vector modes. For example, a triad of the form

$$\mathbf{k}=(0,2,0)=(k_x,0,0)+(-k_x,2,0)=\mathbf{k}_1+\mathbf{k}_2 \tag{5}$$

can transfer power from a pure parallel mode (0,2,0) to a perpendicular mode with different values of k_x.[19] The peak in the power at $w=8$ comes from the Alfvén mode with $k_\parallel=2$ [see panel (a) of Fig. 6]. Similarly, other modes with different values of k_x can also couple to the mode (0,2,0), inheriting some of its wavelike time dependence. The case $k_x=1$ appears as an exception and does not show a clear peak, probably because it is so strongly influenced by the driving, which acts directly on that mode.

Another aspect of the behavior of single wave number modes is to look at the time behavior of the real and imaginary parts of its Fourier amplitudes. This is shown in Fig. 7. If the mode was a single propagating wave, it should describe a circular trajectory in the complex plane, with the angular frequency of this rotation given precisely by the wave frequency. Its actual behavior is much more complex as can be clearly seen in the figure. Panel (a) of Fig. 7 shows the time behavior for a mode with $k_x=0$, $k_y=1$, $k_z=0$, that is, a mode with $\mathbf{k}$ parallel to the mean magnetic field. The trajectory maintains a roughly circular shape due to the existence of the Alfvén wave for that $\mathbf{k}$, however, it fills a broad region in the complex plane than a single wave would do. Evidently its phase is constantly perturbed by nonlinear couplings. Panel (b) of Fig. 6 shows the time behavior for a mode with $k_x=1$, $k_y=0$, $k_z=0$, that is a mode with $\mathbf{k}$ perpendicular to the mean magnetic field (and in the forcing range). The trajectory is quite different from the trajectory of the parallel mode [panel (a)]. This behavior, reminiscent of a random walk, corresponds to the $1/f$ noise type fluctuations observed in the $k=1$ mode.[14]

VI. UNDRIVEN AND WAVE DRIVEN SYSTEMS

One question that might arise is whether the results of the randomly driven system discussed above remain relevant in the absence of driving or with other kinds of forcing. To address this we briefly describe MHD Eulerian spectra computed for representative cases of these types.

First, for the decaying case, without driving, one must consider the effects of fluctuation amplitude that necessarily decreases when viscosity and/or resistivity are nonzero. To account for this in the Eulerian spectrum, prior to carrying out the analysis from the real space time series, we can renormalize the signal at each time using the (square root of) energy computed at that time. This produces a more stationary signal. Figure 8 here shows the result of such an analysis of an undriven run that is otherwise identical in its initial setup to the case shown in Fig. 2. The spectrum is compared in the figure to the corresponding driven case. It is immediately apparent that the basic structure of the Eulerian spectra is similar in the two cases. The wave resonances are broader in the driven case. Both driven and undriven spectra show a tendency toward buildup at low frequencies as described above. The undriven case was run to time $t=100$, thus limiting the lowest frequency that can be analyzed. Running this case much longer that this would lead to a less relevant spectrum, as the system would approach a linear decay regime. For very low energy at late times, even with renormalization,

only a few large scale Fourier modes would contribute to the frequency spectrum. The basic conclusion in this comparison is that the driven and undriven cases are qualitatively similar, with low frequency power very strong in both cases.

Another case of interest might be the driven case in which the energy that is supplied enters the system not randomly, but in the form of Alfvén waves injected either at a boundary or as a body force. This case we examined earlier through reduced MHD simulations, which are weakly three dimensional but support propagating Alfvén wave modes.[15,24] The context of this type of wave driving at the boundary has often been coronal heating driven at the base by Alfvén wave injection. The basic result, not reproduced here,[15] is that the signature in the frequency domain of the wave driving at the base can survive to the top of a coronal model. This occurs even though the spatial information becomes completely scrambled as a Kolmogorov-like cascade is established. We have not quantified the relative dominance of the wave power in the wave driven case compared to the randomly driven cases described in earlier sections above. This is because there are a number of parameters in the open boundary wave driven cases that would require extensive examination to come to firm conclusions. However we suspect that the parameters of the wave driven case can be tuned to relatively favor the wave spectra signatures. This expectation is in part motivated by the possibility of entirely extinguishing turbulence for unidirectional wave driving with no source of counter propagating waves.[15,24] However for strongly turbulent cases of all varieties that we have examined, the wave frequency power does not become the dominant signal.

VII. DISCUSSION AND CONCLUSIONS

We performed numerical simulations of the incompressible MHD equations with a uniform background magnetic field in the regime of turbulence to assess the existence of Alfvén waves in the fluctuations, specifically in the frequency domain. Both the Eulerian frequency spectra and individual wave number mode frequency spectra show the presence of peaks at the corresponding frequencies of the Alfvén modes for full nonlinear simulations in a turbulent regime. However the peaks are much broader and less intense than the peaks obtained from linearized solutions (i.e., Alfvén waves) of the MHD equations. Following individual modes in time shows a much more complex behavior than that could be expected for linear solutions. Nonlinear transfer of energy is also evidenced by the existence of peaks at wave numbers perpendicular to the direction of the mean magnetic field, that would be completely absent in the case of a linear Alfvén mode solution.

Studying the effect of the magnitude of the background magnetic field, it can be concluded that peaks at the wave frequencies are much more clearly seen for large values of the magnetic field (compared to the fluctuating field), as should be expected from the linear approximation in MHD. This can be quantified by the SNR of the Alfven waves peaks. For values of $B_0 \leq 2$ the peaks at the Alfvén frequencies are almost unseen, so less wave type behavior should be expected for fluctuations at moderate values of the mean magnetic field. This would be relevant when the fluctuation and mean are of the same typical magnitude, as they are as for instance in the solar wind.[2]

On the other hand, the comparison of power near Alfvén wave frequency peaks versus the total power in the rest of the frequency spectrum (what we called the WPR) shows that the power at waves is a small fraction of the total power. A very interesting feature is that the WPR appears to have a local maximum near $B_0=2$, an estimate that might be considerably refined with many more long time simulations. For values of B_0 having larger values, the power in the wavelike motions with frequency near the solutions of the dispersion relation actually decreases. The major conclusion of this study is that the frequency spectra of incompressible (periodic, dissipative) MHD, driven at large scales, are dominated by nonlinear effects at all tested values of applied magnetic field strength.

The reason for this behavior, which appears not to have been recognized previously, is that very strong mean magnetic field leads to greater power at very low frequencies, much less than any wave frequencies. Associated with this low frequency power buildup, we also recognized the development of a broad frequency spectrum, with $1/f$ type fluctuations at the low-frequency range (see Ref. 14) and steeper power laws for the high frequency range (at the dissipative region).

Although the peaks in the power at certain frequencies, both in Eulerian spectra and in certain single Fourier mode frequency spectra, indicate the existence of wave-type fluctuations, the present results suggest that the idea of describing MHD turbulence as a superposition of waves remains questionable. For example, for the limited range of mean magnetic field values considered here, we found no parameter range in which the frequency spectra are, in a leading order approximation, given by wave modes at or near the frequencies given by the dispersion relation. The reason for this appears to be, at weak B_0, the dominance of nonlinear couplings at all scales. On the other hand, for very strong $B_0=8$ and above, the effects of anisotropy and the associated buildup of $1/f$ noise at low frequencies begins to dominate the spectra, again swamping the wave effects. Only in an intermediate range of mean field strengths near $B_0=2$ do we find the wave power to be as much as 13% of the power in the frequency domain. Another diagnostic that could in principle detect wavelike behavior is the spectrum of cross helicity.[2,4,7] We carried out such analysis for a number of the runs shown here (now shown) and found no remarkable cross helicity wave signatures.

These results may lead to implications for theoretical treatments of strong MHD turbulence, since they describe, somewhat in detail, the relative importance of waves and turbulence in a particular (and clearly not fully general) instance of MHD turbulence. We have not, for example, examined compressible effects, or any nonclassical features of MHD, such as Hall effect, nor have we examined the influence of widely varying the Reynolds numbers. It is especially unclear to us how to bring the present results into

correspondence with the assumptions underlying perturbation theories known as weak turbulence theories.[10,11,25] It also remains to be seen what the consequences might be for the behavior of charged particles in so-called particle-wave interaction models. For example, can the particle-wave interactions usually invoked in models of particle acceleration[26] be used when a turbulent regime is established? This requires further study, including direct investigation of the response of particles to fully turbulent regimes as compared to the behavior of particles to collections of wave modes that are assumed to obey exact dispersion relations.

ACKNOWLEDGMENTS

P.D. is a member of CIC-CONICET and acknowledges Grant Nos. UBACYT X429/08, ANPCyT PICT 33370/05, and PICT 00856/07. This research was also supported by NASA Grant No. NNX08AI47G (heliophysics theory program), NSF Grant Nos. ATM-0539995 (solar-terrestrial program) and ATM0752135 (SHINE).

[1]For compressible MHD more types of waves appear, the fast and slow magnetoacoustic waves, including velocity fluctuations parallel to wave vectors, i.e., $\mathbf{v_k}\cdot\mathbf{k}\neq 0$.
[2]W. H. Matthaeus and M. L. Goldstein, J. Geophys. Res. **87**, 6011, DOI: 10.1029/JA087iA08p06011 (1982).
[3]A. S. Monin and A. M. Yaglom, *Statistical Fluid Mechanics* (MIT, Cambridge, 1971), Vol. 1, p. 769.
[4]J. W. Belcher and L. Davis, Jr., J. Geophys. Res. **76**, 3534, DOI: 10.1029/JA076i016p03534 (1971).
[5]B. Bavassano, M. Dobrowolny, G. Fanfoni, F. Mariani, and N. F. Ness, Sol. Phys. **78**, 373 (1982).
[6]D. A. Roberts, M. L. Goldstein, L. W. Klein, and W. H. Matthaeus, J. Geophys. Res. **92**, 12023, DOI: 10.1029/JA092iA11p12023 (1987).
[7]M. Dobrowolny, A. Mangeney, and P. Veltri, Phys. Rev. Lett. **45**, 144 (1980).
[8]The condition for interaction of two Alfvénic wave packets, corresponding to "opposite sense of correlation" of **v** and **b**, is sometimes described as "opposite directions of propagation." This is actually misleading and not fully correct. For example, the same condition applies in a two dimensional geometry perpendicular to a uniform mean magnetic field, even though there is, for this case, no propagation along the mean field. Furthermore, the condition for interaction of the packets also applies when there is no mean magnetic field and, therefore, no propagation.
[9]R. Kraichnan, Phys. Fluids **8**, 1385 (1965).
[10]S. J. Schwartz, Mon. Not. R. Astron. Soc. **178**, 399 (1977).
[11]S. Galtier, S. V. Nazarenko, A. C. Newell, and A. Pouquet, J. Plasma Phys. **63**, 447 (2000).
[12]Y. Zhou, W. H. Matthaeus, and P. Dmitruk, Rev. Mod. Phys. **76**, 1015 (2004).
[13]V. N. Tsytovich, *An Introduction to the Theory of Plasma Turbulence*, 1st ed. (Pergamon, New York, 1972), p. 1.
[14]P. Dmitruk and W. H. Matthaeus, Phys. Rev. E **76**, 036305 (2007).
[15]P. Dmitruk, W. H. Matthaeus, and L. Lanzerotti, Geophys. Res. Lett. **31**, L21805, DOI: 10.1029/2004GL021119 (2004).
[16]H. Tennekes, J. Fluid Mech. **67**, 561 (1975).
[17]S. Y. Chen and R. H. Kraichnan, Phys. Fluids A **1**, 2019 (1989).
[18]A. R. Bulsara and L. Gammaitoni, Phys. Today **49**, 39 (1996).
[19]J. Shebalin, W. H. Matthaeus, and D. C. Montgomery, J. Plasma Phys. **29**, 525 (1983).
[20]S. Oughton, E. R. Priest, and W. H. Matthaeus, J. Fluid Mech. **280**, 95 (1994).
[21]D. C. Robinson and M. G. Rusbridge, Phys. Fluids **14**, 2499 (1971).
[22]J. W. Bieber, W. Wanner, and W. H. Matthaeus, J. Geophys. Res. **101**, 2511, DOI: 10.1029/95JA02588 (1996).
[23]A. Alexakis, B. Bigot, H. Politano, and S. Galtier, Phys. Rev. E **76**, 056313 (2007).
[24]L. del Zanna and M. Velli, Adv. Space Res. **30**, 471 (2002).
[25]B. D. G. Chandran, Phys. Rev. Lett. **95**, 265004 (2005).
[26]J. A. Miller, P. J. Cargill, A. G. Emslie, D. G. Holman, B. R. Dennis, T. N. LaRosa, R. M. Winglee, S. G. Benka, and S. Tsuneta, J. Geophys. Res. **102**, 14631, DOI: 10.1029/97JA00976 (1997).